Effect of Polymerization Temperature on the Morphology and Electrooptic Properties of Polymer-Stabilized Liquid Crystals

C. V. Rajaram and S. D. Hudson*

Department of Macromolecular Science, Case Western Reserve University, Cleveland, Ohio 44106

L. C. Chien

Liquid Crystal Institute, Kent State University, Kent, Ohio 44242

Received October 31, 1995. Revised Manuscript Received June 20, 1996[⊗]

The effect of structure of mesogenic diacrylate monomer and temperature of photopolymerization on the morphology of polymer networks has been studied in detail. Increasing the temperature of photopolymerization increases the size of the constituent units and correspondingly the size of the pores of the polymer network. A model explaining the dependence of the characteristic dimension of the polymer network on the concentration and the relative rates of diffusion and reaction has been developed. A new type of morphology consisting of a network of plates was made from a smectogenic monomer (4,4′-bis{4-[6-(acryloyloxy)hexyloxy]benzoate}biphenylene) and demonstrated to have unusual electrooptic properties. Electrooptic studies were performed on all the morphologies obtained. Morphologies having highly oriented structure result in higher threshold voltage and switching hysteresis.

Introduction

Low-molar-mass liquid crystal−polymer dispersions are being studied intensively for their potential for applications such as privacy windows, high-intensity light-shutter valves, large-area flat-panel displays, etc. One such type of material is the polymer-stabilized liquid crystals (PSLC) in which the monomers are dissolved in a low-molar-mass liquid crystal, aligned in a suitable display state, and photopolymerized.[1] These polymers are generally dispersed in small amounts (typically 3 wt %) in conventional liquid crystals to improve the electrooptic properties of existing devices. The polymer networks formed in such systems containing mesogenic monomers have been extensively studied.[2−7] The PSLC displays have better viewing angle, shorter response times, and bistability, unlike conventional liquid-crystal displays.[8] A dynamic light-scattering study of the polymer-stabilized liquid-crystal monodomains has demonstrated that the polymer network has substantially increased the twist elastic constant and viscosity of the low-molar-mass liquid-crystal solvent.[9] Increasing the polymer concentration in PSLC causes an increase in the response times.[10] The polymer-modified twisted nematic devices have been reported to have significantly lowered the threshold voltage.[11] Also, these polymer networks have eliminated the striping texture at high twist states of supertwisted birefringent-effect devices or supertwisted nematic devices.[12] Polymer-stabilized cholesteric formulations (PSCT) whose planar state reflects across the entire visible spectrum thus producing a black-on-white image have also been made.[13]

All the recent work done on these PSLCs suggests that the performance of the devices relates to the morphology of the polymer network. Recently, the morphology of these polymer networks[5] and its evolution during photopolymerization in these PSLCs are reported.[14] The object of this paper is to demonstrate the effect of temperature of photopolymerization on the morphology of these polymer-stabilized liquid crystals, and its effect on the electrooptic properties as studied from the change in the transmission of laser light through a reverse-mode cell as a function of applied voltage.

Experimental Section

Sample Preparation. Samples were prepared by dissolving 3 wt % concentration of diacrylate monomers 4,4′-bis-

[⊗] Abstract published in *Advance ACS Abstracts,* September 1, 1996.

(1) Yang, D. K.; Doane, J. W. *SID Techn. Paper Digest XXIII* **1992**, 759.
(2) Hikmet, R. A. M. *Liq. Cryst.* **1991**, *9*, 405.
(3) Hikmet, R. A. M. *Mol. Cryst.* **1991**, *198*, 357.
(4) Hikmet, R. A. M.; Higgins, J. A. *Liq. Cryst.* **1992**, *12*, 831.
(5) Hikmet, R. A. M. *J. Appl. Phys.* **1990**, *68*, 4406.
(6) Hikmet, R. A. M.; Zwerver, B. H. *Mol. Cryst.* **1991**, *200*, 197.
(7) Hikmet, R. A. M.; Zwerver, B. H. *Mol. Cryst., Liq. Cryst.* **1992**, *12*, 319.
(8) Yang, D. K.; Chien, L. C.; Doane, J. W. *Appl. Phys. Lett.* **1992**, *60*, 3102.
(9) Gu, D. F.; Jamieson, A. M.; Chien, L. C. *Techn. Reports ALCOM Symp.* **1994**, 101.
(10) Fung, Y. K.; Sun, Y.; Pfeiffer, M. T. P.; Yang, D. K.; Doane, J. W. *Techn. Reports ALCOM Symp.* **1994**, 52.
(11) Bos, P. J.; Rahman, J. A.; Doane, J. W. *SID Digest Techn. Papers XXIV* **1993**, 887.
(12) Fredley, D. S.; Quinn, B. M.; Bos, P. J. *Techn. Reports ALCOM Symp.* **1994**, 19.
(13) West, J. L.; Magyar, G. R.; Francl, J. J.; Nixon, C. M. *Techn. Reports ALCOM Symp.* **1994**, 43.
(14) Rajaram, C. V.; Hudson, S. D.; Chien, L. C. *Chem. Mater.* **1995**, *7*, 2300.
(15) Yang, D. K.; Chien, L. C.; Doane, J. W. *Proc. Soc. Info. Display XXIV* **1992**, 887.

S0897-4756(95)00520-5 CCC: $12.00

4, 4' - bis(acryloyloxy)biphenyl (BAB)

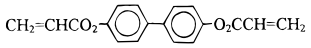

4, 4' - bis[6-(acryloyloxy)hexyloxy]biphenyl (BAB6)

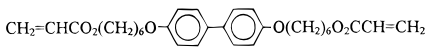

4,4' - bis{4-[6-(acryloyloxy)hexyloxy]benzoate}biphenylene (BABB6)

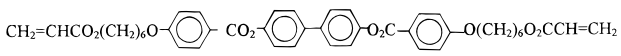

benzoin methyl ether (BME)

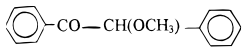

4'-pentyl 4-biphenyl carbonitrile (5CB)

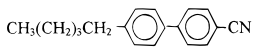

E48 - Eutectic mixture of several low-molar-mass liquid crystals [16]

Figure 1. Structure of all the chemicals used in this study.

(acryloyloxy)biphenyl (**BAB**), 4,4′-bis(6-(acryloyloxy)hexyloxy)-biphenyl (**BAB6**), or 4,4′-bis{4-[6-(acryloyloxy)hexyloxy]-benzoate}biphenyl (**BABB6**), and a small amount (0.3 wt %) of photoinitiator benzoin methyl ether (**BME**) into a common low-molar-mass liquid-crystal solvent, **E48**, a eutectic mixture of several similar low-molar-mass liquid crystals.[16] In some cases, the solvent was a single component, namely, 4′-pentyl-4-biphenylcarbonitrile (**5CB**). The nematic-to-isotropic phase transition temperature for the liquid-crystal solvents, **E48** and **5CB**, were measured to be 87 and 35.2 °C, respectively. The addition of 3% of monomers **BAB**, **BAB6**, and **BABB6** to the liquid-crystal solvents lowered the nematic-to-isotropic phase-transition temperature to between 2 and 3 °C. Synthesis of the monomers and photoinitiator has been described previously,[1,8,15] and the structures for all the chemicals used are given in Figure 1. The solution (monomer dissolved in appropriate solvent) was then sandwiched between properly treated glass slides. The glass slides had been spin-coated with polyimide precursor solution (oligomeric polyimide DuPont 2555 mixed with a thinner), cured for an hour at 250 °C, and then buffed unidirectionally for obtaining a homogeneous boundary condition. For cells prepared for morphological examination, Mylar spacers of approximately 12.5 μm thickness were used to control the thickness of the cell. For electrooptic characterization, more stringent control of the thickness is required and 15 μm glass spacers were used. The glass spacers were sprayed on the treated glass and then were assembled in a class 100 clean room. The cell was then sealed on all sides with epoxy mixture in order to create a near-inert condition for the subsequent photopolymerization. The samples were irradiated for 20 min with UV light of 365 nm wavelength and intensity of 1.75 mW/cm^2. The temperature of the sample was controlled using a Mettler hot stage. The morphology of these cells was checked and found to reproduce findings from the previous cells, which used Mylar spacers.

Morphology Examination. Uniform homogeneous alignment of the LC director was confirmed by cross-polarized light microscopy. The image was black when the rubbing direction was parallel to either polarizer or analyzer. A uniformly bright image was formed when the specimen was rotated to oblique angles. The specimen preparation for electron microscopy was as follws:

The cell after exposure to UV light was fractured at the edges and immersed in hexane for 2 days. The solvent leaches out the low-molar-mass liquid crystal, leaving the bare polymer network on the glass slide. This can be confirmed by polarized light microscopic examination. The cell is then delicately split open when dry and coated with a 90 Å thick layer of gold using a Biorad-Polaron Divisions' SEM coating system. The morphology of these samples was then observed using a JEOL JSM 840 scanning electron microscope operated at 25 kV in secondary electron imaging mode. In situ examination of the cell by polarized light microscopy suggests that the sample preparation procedure for SEM does not significantly affect the morphology.[17]

(16) Allen, F. private communication.

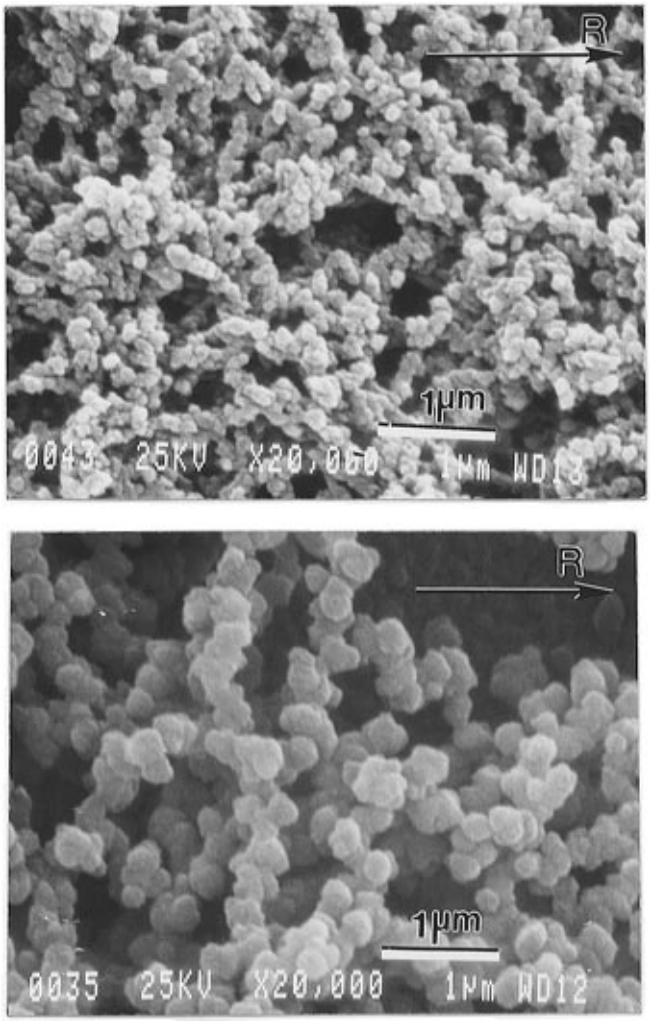

Figure 2. SEM micrograph of a homogenous cell containing 3% **BAB** in **E48** polymerized at (a) 28 and (b) 75 °C. R denotes the rubbing direction. The scale bar in each case is 1.0 μm.

Electrooptic Measurements. The electrooptic properties of these cells were studied by measuring the transmittance of the model display cell with a He−Ne laser light. The collection angle of the detector was 2°. The detector is calibrated by checking for zero signal with the laser off. Then the cell is placed in the line of the detector and the orientation is adjusted to get maximum signal detection at zero field. The voltage is increased at the desired rate and the intensity of the laser light automatically recorded into the computer.

Results and Discussion

Morphology Study. For monomers, without a flexible spacer between the rigid core and the polymerizable moiety, there is excessive coupling between the motion of the backbone and the motion of the mesogen, and such polymers do not form liquid crystalline phases.[18] Consequently, a beadlike morphology results from the photopolymerization of **BAB**.[14] The beads in such a morphology are nodular and aggregated into a loose network with pores ranging in size and shape. More

(17) Muzic, D. S.; Rajaram, C. V.; Hudson, S. D.; Chien, L. C. *Polym. Adv. Technol.*, in press.

(18) Finkelmann, H.; Ringsdorf, H.; Wendorff, J. H. *Makromol. Chem.* **1978**, *179*, 273.

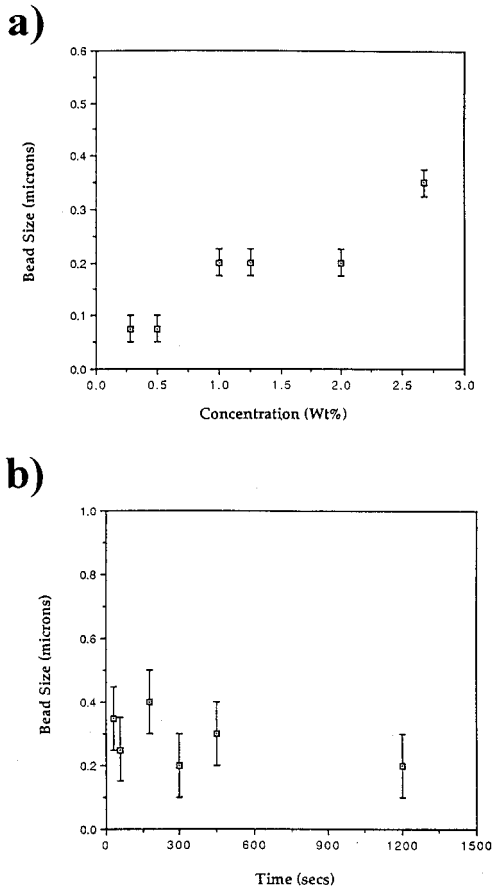

Figure 3. (a) Effect of monomer concentration of **BAB** in **5CB** on the nodular bead size polymerizing under similar conditions (nematic conditions with 8 mW/cm^2 intensity UV light). (b) Effect of conversion on the bead size of 3% **BAB** solution in **5CB** polymerized in nematic conditions exposed to UV light of intensity 8 mW/cm^2.

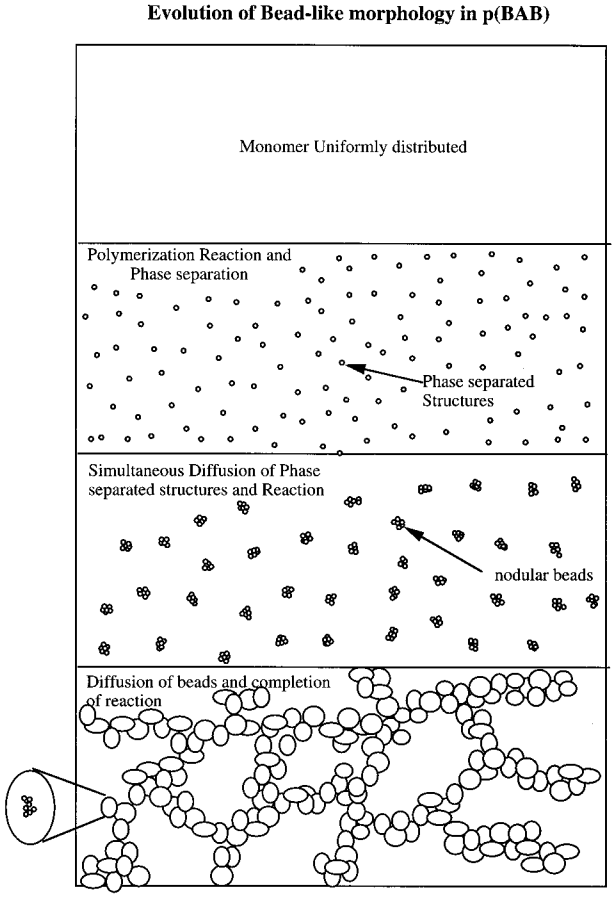

Figure 4. Schematic representation of morphology evolution in polymer stabilized liquid crystals of p(**BAB**).

can be learned about the network formation and aggregation processes by varying monomer concentration, polymerization temperature, and extent of reaction. (It is advantageous to examine **BAB** networks, since the morphology is always beadlike, and characterization of the bead size by SEM is straightforward.) Increasing concentration causes an increase in the bead size (Figure 3a), whereas increasing conversion does not (Figure 3b). This suggests that the nodular beads are formed within the first 30 s and that subsequent increases in conversion are accomplished mostly within the nodular beads. The bead size depends significantly on polymerization temperature (Figure 3). When **BAB** is polymerized in **E48** at 28 °C, nodular beads comprising the network are approximately 0.2 ± 0.1 μm. The morphology at higher temperature (75 °C) is similar, yet the beads are less nodular and larger, ~0.4 ± 0.1 μm in size. Correspondingly, the pores of the network are larger than those formed at lower polymerization temperatures.

These changes in network morphology can be understood based upon kinetic model, presented below. We hypothesize that the size of nodular beads, and in turn the final morphology, is determined by a balance between the rates of reaction and of bead diffusion. Ideally, the process or morphology evolution in the case of **BAB** monomers may be depicted as in Figure 4, though the processes mentioned might occur at different rates in different regions of the sample, generating fixed fluctuations in the density of the network. Initially, the monomers are uniformly distributed in the liquid-crystalline solution. When the UV lamp is turned on, there is initiation of polymerization over the entire sample. The monomers migrate from the vicinity and feed the polymerization reaction. As the monomers are being rapidly used up, the polymer molecules eventually reach a sufficiently high molecular weight and/or branch content, and they phase separate from the solvent (Figure 4a). These primary polymer-rich particles, observed previously[14] after very short polymerization times and low monomer concentration, contain many reactive moieties, a substantial fraction of which are on the surface. These react with other active surface sites on other particles. As the particles grow in size, they become more sluggish, so that eventually the reaction of the surface moieties of different phase separated particles is diffusion-limited. This process leads to final network morphology of the beads.

On the basis of this model, the characteristic size of the nodular beads depends on condition of crossover from reaction-limited to diffusion-limited growth. Since the early 1980s, two types of aggregation processes have been identified: reaction-limited and diffusion-limited.[19−21] For a given system undergoing aggregation, one of these two processes may occur. These may be distinguished by the compactness of the aggregate,

(19) Kolb, M.; Jullien, R. *J. Phys. Lett.* **1984**, *45*, L977.
(20) Family F,; Meakin, P.; Viesek, T. *J. Chem. Phys.* **1985**, *83*, 4144.
(21) Weitz, D. A.; Huang, J. S.; Lin, M. Y.; Sung, J. *Phys. Rev. Lett.* **1985**, *54*, 1416.

which may be characterized by its fractal dimension. Reaction-limited aggregates are compact, having fractal dimensions in excess of 2. This compares with a fractal dimension of approximately 1.6−1.8 for less dense diffusion-limited aggregates. It has also been pointed out that reaction-limited aggregation processes can, if allowed to continue, become eventually diffusion-limited. This crossover can occur if there is a fixed amount of aggregating species, which are more likely to react and become more sluggish in their movement as their size increases.[19−22] We extend these ideas to develop an expression for a characteristic dimension of the final network. At early times, particles are small and close together and the growth is limited by the time for two particles to react with one another, τ_{rxn}. The diffusion time is given by $X^2/D_{particle}$, where X is the average distance between particles and $D_{particle}$ is the diffusion coefficient for the particle or nodular bead of size r. Since the concentration (ϕ) of polymer (monomer units) is constant, the number density, and size, of particles varies to maintain ϕ:

$$\phi = (1/X^3)(^4/_3\pi r^3) \quad (1)$$

Rearranging eq 1 for the average distance between the diffusing particles X is

$$X \sim (\phi)^{-1/3}(^4/_3\pi)^{1/3} r \quad (2)$$

From Einstein's hydrodynamical theory

$$D_{particle} \sim kT/\eta r \quad (3)$$

where k is the Boltzmann constant, T is the temperature, η is the viscosity of the medium, and r is the radius of the diffusing particle. The diffusion time can now be expressed using eqs 2 and 3:

$$\tau_{diff} \sim [(\phi)^{-2/3} r^3 \eta] kT \quad (4)$$

Therefore the diffusion slows markedly as the particle grows in size. The time for two particles to react with one another is inversely related to the rate of the cross-linking reaction:

$$\tau_{rxn} \sim 1/R_X \quad (5)$$

The crossover from reaction-limited to diffusion-limited aggregation is defined when τ_{diff} and τ_{rxn} are equivalent. The radius defined by this condition is therefore the size, ξ, of the nodular beads (neglecting internal shrinkage) characteristic of the final network. Replacing ξ for r in eq 4 and combining with eq 5 gives, after rearrangement

$$\xi \sim (kT/\eta R_X)^{1/3} (\phi)^{2/9} \quad (6)$$

Photocalorimetric measurements demonstrate that the reaction rate does not depend strongly on temperature, so that the strongest temperature dependence is with η. Thus as temperature increases, ξ is expected to increase, as observed. We are conducting experiments to further test this model.

The above-mentioned model applies for all cross-linking monomers (with or without flexible spacers) that do not gel before phase separation. These instead separate as microgels and the final macroscopic network is formed only after diffusion and reaction of these particles. The morphology can then be related to monomer concentration, the rate of polymerization, and the solvent viscosity. Moreover, the morphology of anisotropic systems will be influenced by anisotropic diffusion, yet the crossover between reaction-limited and diffusion-limited aggregation applies in general.

Our previous results show that the morphology of **BAB** is always beadlike while that of **BAB6** depends on whether the solvent is nematic or isotropic. When **BAB6** is photopolymerized in the nematic phase, a fibrous network develops, yet polymerization in the isotropic phase produces a beadlike morphology.

Previous work on the morphology of **BAB6** in **5CB**[14] suggested that the fibrous morphology observed is due to the flexible spacers preserving the orientation of the mesogens in the polymer network, inspite of the disruption of nematic order caused by covalent cross-links between monomers due to photopolymerization. This forms fairly anisotropic phase-separated structures. The anisotropic aggregation and shrinkage of these phase separated structures are responsible for fiberlike morphology of this system.[14]

Morphology of **BAB6** polymerized in **E48** at 28 °C (Figure 5a) is fibrillar in nature with smooth fibers about 0.1 μm in thickness well aligned along the rubbing direction. Increasing the temperature of photopolymerization to 80 °C (Figure 5b) causes the fibers to be rougher, more thicker (0.3 ± 0.1 μm), and well aligned along the rubbing direction. Further increase in temperature to 90 °C results in a markedly different, network of quasi-platelike morphology (Figure 5c) with plates about 0.5 μm in breadth and 0.1 μm in thickness without any orientation leading to large-pore structure. When polymerized at still higher temperatures (120 °C in isotropic state, Figure 5d), the morphology is simply an aggregation of small beads (smaller than **BAB** in **5CB**[14] at isotropic state) probably due to increased rate of initiation of photopolymerization (arising from additional initiation of polymerization due to thermal initiation at these high temperatures).

To summarize the results of Figure 5, increasing the temperature of photopolymerization of **BAB6** gradually changes in fiberlike morphology to beadlike morphology of **BAB**.[14] Increasing the photopolymerization temperature increases the roughness of the fibers which might be due to several factors: decreased order parameters of the solvent, more isotropic diffusion of monomers and phase-separated structures, and segregation of the components of the solvent mixture in the polymer-rich phase. The larger diameter of the fibers formed at 80 °C is consistent with the particle diffusion considerations described for **BAB**. At 90 °C, quasi-platelike structures are formed possibly due to the smectic like order in the polymer-rich phase, made possible by the segregation of different components of the solvent mixture. But at high temperatures (120 °C) small beadlike structures are formed due to the isotropic state of the polymerizing medium but the origins of the small size of these beads are not clearly understood.

So far we have considered the reaction, diffusion limitations and the effect of anisotropy of the liquid-crystal solution on the morphology of the polymer

(22) Asnaghi, D.; Carpineti, M.; Giglio, M.; Sozzi, M. *Phys. Rev.* **1993**, *A45*, 1018.

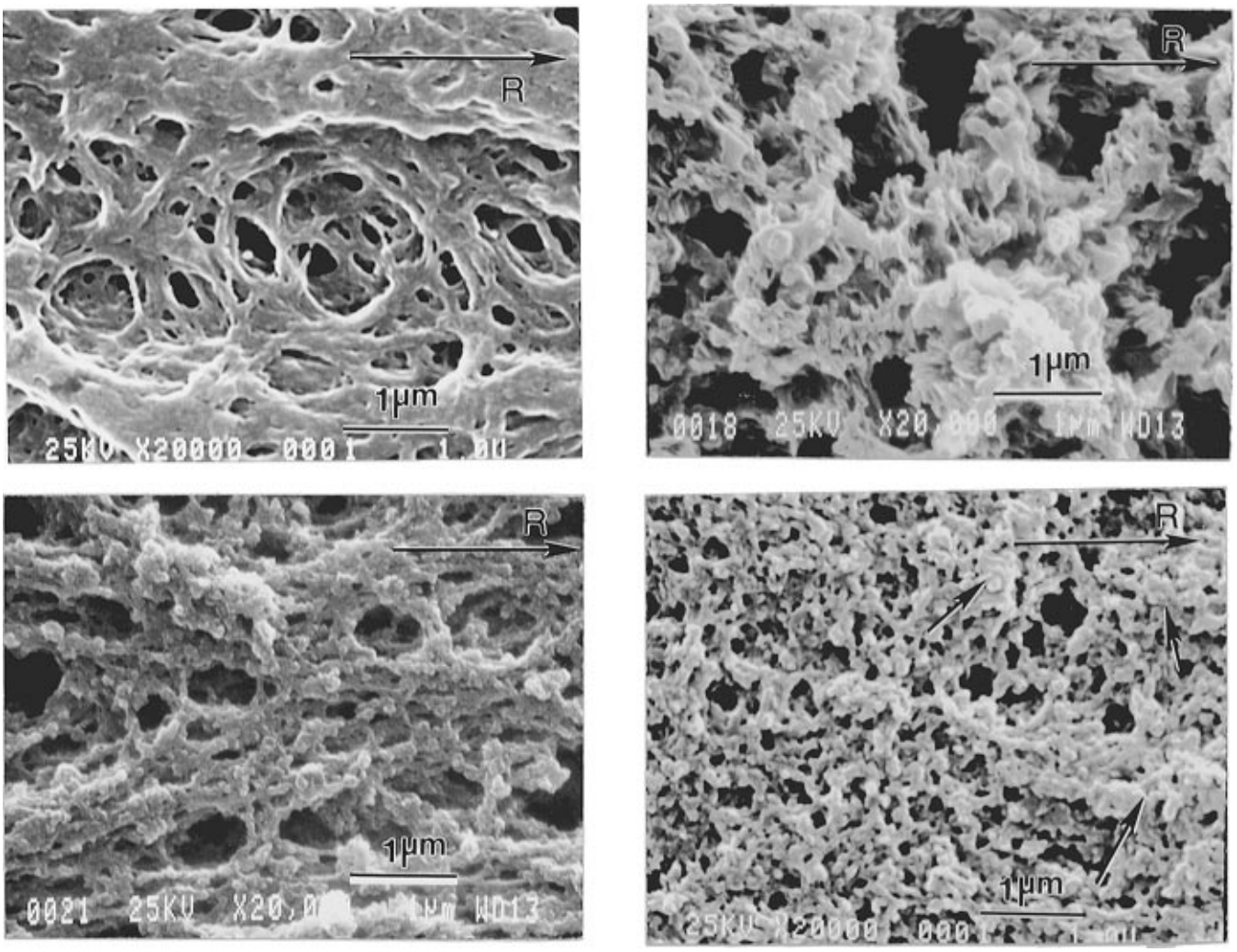

Figure 5. SEM micrograph of a homogeneous cell containing 3% **BAB6** in **E48** polymerized at (a, top left) 28, (b, bottom left) 80, (c, top right) 90, and (d, bottom right) 120 °C. R denotes the rubbing direction. All micrographs are printed at same magnification. The scale bar in each case is 1.0 μm.

network in PSLC. Along with the above, now we consider the effect of the size of the mesogenic core on the morphology of the polymer network. We chose monomer **BABB6** which is similar to **BAB6** except that the mesogen is just over twice the size of the biphenylic mesogen of **BAB6**. We assume that the increase in the length of the mesogen would change the orientational and positional order characteristic of the polymer-rich phase. As a result several morphological changes are observed. In contrast to the previous monomers, **BABB6** is itself liquid crystalline. This monomer exhibits a smectic phase between 102.5 and 121.1 °C which might be responsible for some of the unique morphology of these polymer-stabilized liquid crystals, discussed below.

The morphology of **BABB6** photopolymerized in **E48** at 28 °C (Figure 6a) is fibrillar with rough and thick fibers about 0.3 ± 0.1 μm in diameter. Some fibers have agglomerated into much thicker strands with pores that vary in size and shape. This morphology is similar to **BAB6** photopolymerized in **E48** at a higher temperature at 80 °C. Increasing the temperature of photopolymerization to 75 °C (Figure 6b) results in a beadlike network interspersed with platelike structures. The beads are nodular (0.3 ± 0.1 μm in size) and have aggregated into a network resulting in pores of varying size and shape. The interspersed plates, are irregular, twisted and bent of various size (2−8 μm in size and less than 0.2 μm in thickness) and shape. Both the beads and the plates lack any orientation. Further increase in temperature of photopolymerization to 95 °C results in a morphology equally dominated by the plates (1−2 μm in size and 0.2 μm in thickness) and thick smooth disks of uniform size (0.4 μm in size and0.2 μm in thickness) and shape (Figure 6c). The plates are all interconnected. Photopolymerization at a much higher temperature of 140 °C results in an interconnected platelike morphology with plates ranging in orientation and size. The size varies from less than a micron to several microns, the thickness of all these plates remains always less than 0.2 μm.

It seems that the longer mesogenic monomer, being more likely to form the smectic phase forms roughened and platelike morphologies more readily and at lower temperatures than the smaller **BAB6** suggesting that the major factor for roughening of the fibers of **BAB6** at 80 °C is its tendency to form platelike morphology. To understand why fibers (presumably nematic like) are formed at the lower temperature, we suggest that insufficient mobility exists within the polymer-rich phase to form the layered structure. Thus the structure characteristic of the initially less concentrated polymer-rich phase is frozen-in.

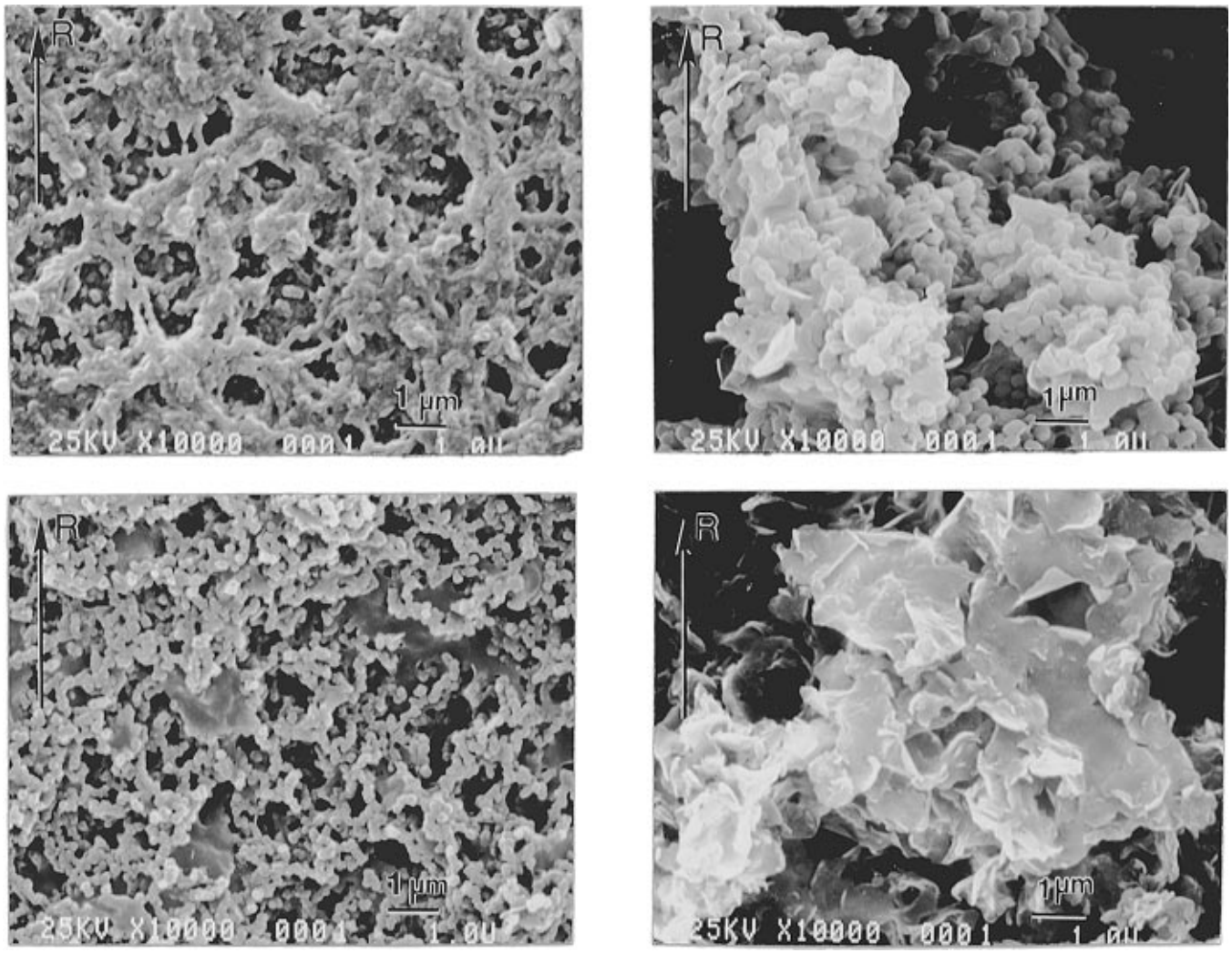

Figure 6. SEM micrograph of a homogeneous cell containing 3% **BABB6** in **E48** polymerized at (a, top left) 28, (b, bottom left) 75, (c, top right) 95, and (d, bottom right) 140 °C. R denotes the rubbing direction. The scale bar in each case is 1.0 μm.

At a much higher temperature of 140 °C, the polymerization temperature is possibly higher than the glass transition temperature of the polymer network, because the polymer network phase apparently separates as small platelike structures, which then aggregates into a platelike morphology. Similar platelike morphology is observed at varying conversions from very low (exposure to UV light for 1 min) to high conversion (exposure to UV light for over 20 min), suggesting that there is sufficient mobility inside the polymer network to rearrange into layered platelike structures upon phase separation. These platelike structures aggregate into a network of plates by an apparently diffusion-limited aggregation process.

Electrooptic Properties of Polymer Stabilized Liquid Crystals. Since the major targeted application of these polymer-stabilized liquid crystals is as display devices, we studied the effect of applied voltage on the transparency of the model display cell of 15 μm thickness. Typically, in a reverse-mode cell of the polymer-stabilized liquid crystals,[23] as the voltage applied normal to the cell increases there is initially no change in the transparency of the cell and, after a particular threshold voltage, the cell starts to gradually decrease in transparency becoming opaque. The threshold voltage in the voltage when the cell starts to switch from clear to opaque. The cell remains at nearly constant opacity on further increase in applied voltage. Increasing voltage much higher, the LC progressively becomes oriented along the field direction and the cell becomes less opaque. In our study, we focus only on the switching behavior from the clear to opaque state at low applied voltages.

The model for the electrooptic behavior of a typical reverse mode cell is shown in Figure 7. Initially at zero-field the cell appears clear because director deviations away from the rubbing direction are small and the optical properties of the polymer and the liquid-crystal solvent are similar. On application of voltage normal to the cell, it gradually becomes opaque due to the competition between two processes: namely, the low-molar-mass liquid-crystal solvent tending to align along the direction of the applied field (positive dielectric anisotropy) and the prevention of this alignment, in some domains, by the polymer network. This inhomogeneous orientation of the low-molar-mass liquid-crystal solvent causes scattering of incident light (white state). The reorientation of the LC in some domains is prevented by the immobility of the polymer and the

(23) A reverse-mode cell is usually made out of indium−tin oxide coated glass over which is spin-coated a thin layer of polyimide and rubbed. This creates a homogeneous boundary condition and the monomer solution is photopolymerized without the application electric field.

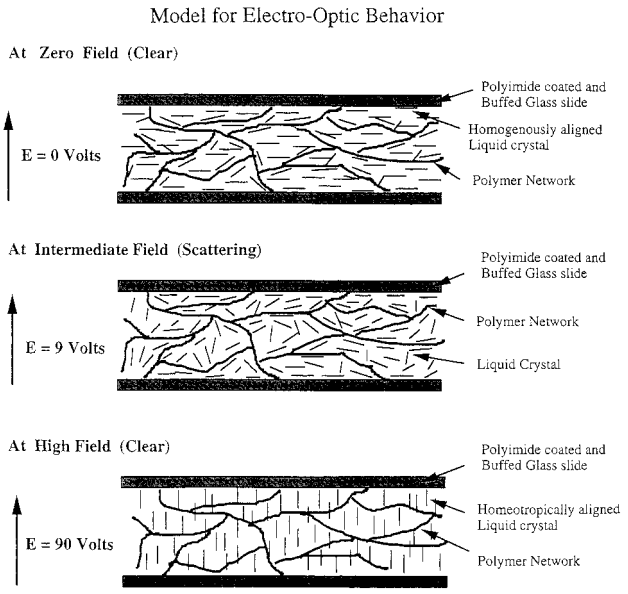

Figure 7. Schematic representation of the switching process in the reverse mode polymer stabilized liquid-crystal cells.

anchoring of the LC orientation at the interface of these phase separated structures. The cooperativity of the liquid-crystal molecules in the nematic state (i.e. director stiffness) extends this misalignment to distances greater than the molecular scale. At sufficiently high applied electric field, director stiffness and anchoring are insufficient and most of the liquid-crystal solvent molecules will align homeotropically along the direction of applied field and the cell would become clear again.[1]

Typically a reverse-mode display cell is characterized mainly for its threshold voltage (voltage at which the cell switches from the clear state to a scattering state) and contrast [ratio of the percent transmission of the "OFF" (clear) and "ON" (scattering) states]. Hysteresis, or the lack of reversible switching is also important. In this paper, we are considering the effect of morphology of the polymer network on these important display characteristics. We begin by studying the electrooptic properties due to a simple beadlike morphology of **BAB**, and we explore the effect of increasing the bead size.

Effect of p(BAB) on the Electrooptic Properties of Polymer-Stabilized Liquid Crystals. The electrooptic properties of the reverse-mode polymer-stabilized liquid crystals due to the monomer **BAB** is shown in Figure 8. Figure 8a shows the electrooptic curve for the reverse-mode cell of monomer **BAB** polymerized at 28 °C. As we increase the voltage applied across the cell, there is initially very little change in the transparency of the cell (~85% transmission) until the voltage reaches 7 V when the cell begins to switch to a scattering state reaching a low steady state value of transparency at about 15 V. On decreasing the voltage, the cell changes reversibly from scattering state to a much more transparent state exhibiting hysteresis. The contrast of this cell is low (about 0.3) and could be greatly enhanced by adding a chiral agent. The presence of hysteresis suggests that the LC molecules follow a route to orient themselves when the voltage is increased which is different from the one followed, when the voltage is decreased.[24] In the scattering state

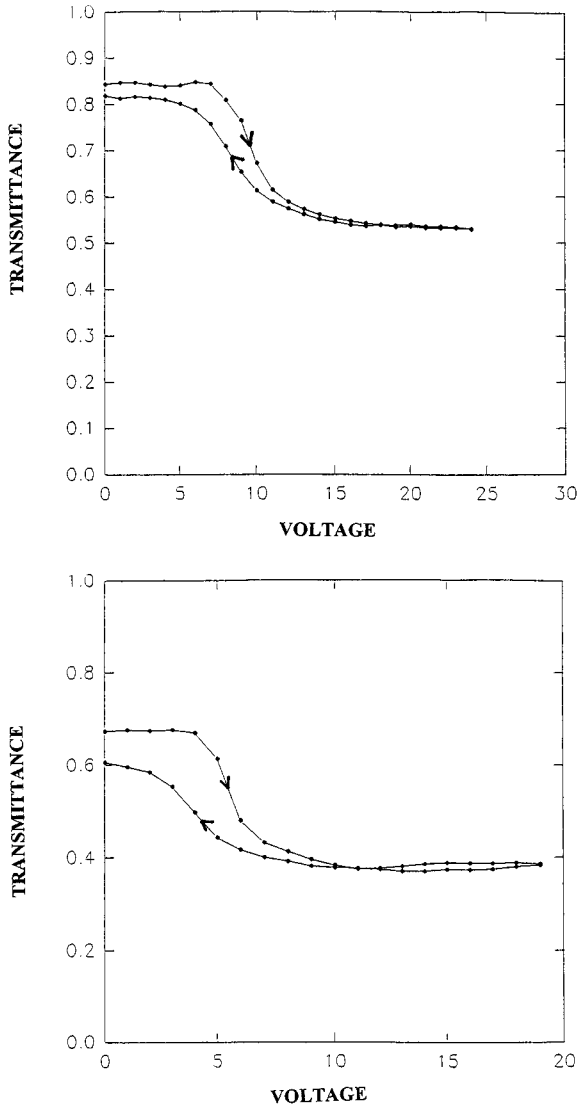

Figure 8. Electrooptic properties of a reverse mode cell of 15 μm thick containing polymer stabilized liquid crystals of **BAB** polymerized in **E48** at (a, top) 28 and (b, bottom) 75 °C.

(multidomain nematic state), the domains need not be bounded by polymer on all sides. Therefore hysteresis could be suggested as caused by the frustration of the nematic director at the domain boundaries on decreasing the applied voltage to the cell.[24]

Figure 8b shows the electrooptic curve of the reverse-mode cell due to **BAB** monomer polymerized at 75 °C. The general characteristics of the curve remains the same, but the threshold voltage has dropped to 4 V and a much lower initial transparency at zero-field (70% transmission). Increasing the size of the beads does not seem to have any significant impact on the contrast or the hysteresis of the cell. However, two other effects are apparent. Increased bead size suggests greater disruption of the initial LC director and increasing scattering resulting in lower transparency at zero-field. Second, the decrease in the threshold voltage may be attributed to the increase in pore size of the polymer network. As the bead size increases, the average distance between beads and the corresponding pore size of the polymer network must also increase. Moreover, increased disruption of the LC director also reduces the threshold voltage.

(24) Hikmet, R. A. M.; Boots, H. M. J. *Phys. Rev. E* **1995**, *51*, 6A, 5824.

Effect of p(BAB6) on the Electrooptic Properties of Polymer-Stabilized Liquid Crystals. Owing to the greater network anisotropy associated with **BAB6** stronger interaction between the LC solvent and polymer network and corresponding changes in electrooptic properties are expected. Figure 9a shows the electrooptic curve of a reverse-mode cell of **BAB6** polymerized at 28 °C. The initially transparent cell (82% transmission) on application of electric field starts to switch at a threshold voltage of 8 V and reaches a steady opaque state around 17 V with a large hysteresis and contrast of about 0.4. For a similar cell polymerized at 80 °C, there is no significant difference in the electrooptic characteristics of the cell to that polymerized at lower temperature. But on further increasing the temperature of polymerization (90 °C), we observe a much different electrooptic response as shown in Figure 9b. The threshold voltage of the cell has dropped dramatically to 2 V with a much lower transparency at zero-field and a low contrast of about 0.3. The electrooptic curve is much steeper than the curves obtained at lower temperature. Continued application of voltage to this cell causes a gradual increase in the transparency of the cell with a large hysteresis. Figure 9c shows the electrooptic response of the cell polymerized at 120 °C. The electrooptic properties of this cell are similar to the cell polymerized with the monomer **BAB** with a threshold voltage of about 4 V and a lower contrast of 0.3. On reversing the voltage it regains most of its transparency with a small hysteresis.

From these results, a number of differences in comparison to **BAB** are apparent. First, the greater orientation of fibrous **BAB6** networks causes a much higher threshold, indicating a much more efficient coupling between the orientation of the polymer network and the LC solvent. Interestingly, the changes in the roughness of the fibers (evident from comparison of SEM of networks polymerized at 28 and 80 °C) do not significantly influence device performance. When the orientational order within the polymer is reduced, the network consists of disordered, rough platelike structures, and the threshold is drastically reduced. The lower contrast of this system can be attributed to the decreased transparency of the cell at zero-field because of large plates oriented randomly in all directions. Another peculiar feature is that there is a gradual increase in the transparency of the cell after it has reached the highest opaque state. This indicates that, gradually, a smaller fraction of the LC solvent is disrupted away from the orientation of the electric field by the polymer. This could be achieved at high voltages only if the anchoring energy of the LC solvent is weaker for the platelike morphology. As we further increase the temperature of polymerization to 120 °C into the isotropic state of these materials, we get the beadlike morphology when the electrooptic response of the cell is similar to that polymerized at lower temperatures but with the lower threshold voltage of 4 V and a small hysteresis. To further understand the effect of unique platelike morphology on the electrooptic properties of the single-pixel model display cell, we investigated systems with more well-defined plates, such as found in PSLCs prepared with **BABB6**.

Effect of p(BABB6) on the Electrooptic Properties of Polymer-Stabilized Liquid Crystals. The

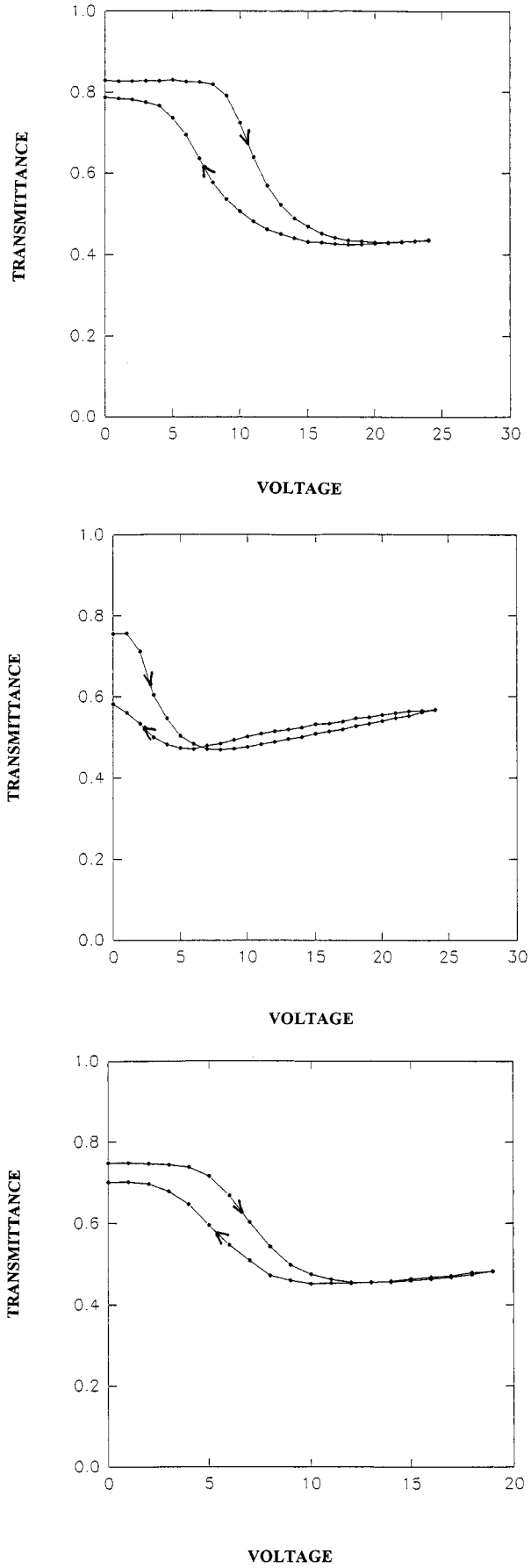

Figure 9. Electrooptic properties of a reverse mode cell of 15 μm thick containing polymer stabilized liquid crystals of **BAB6** polymerized in **E48** at (a, top) 28, (b, middle) 90 °C and (c, bottom) 120 °C.

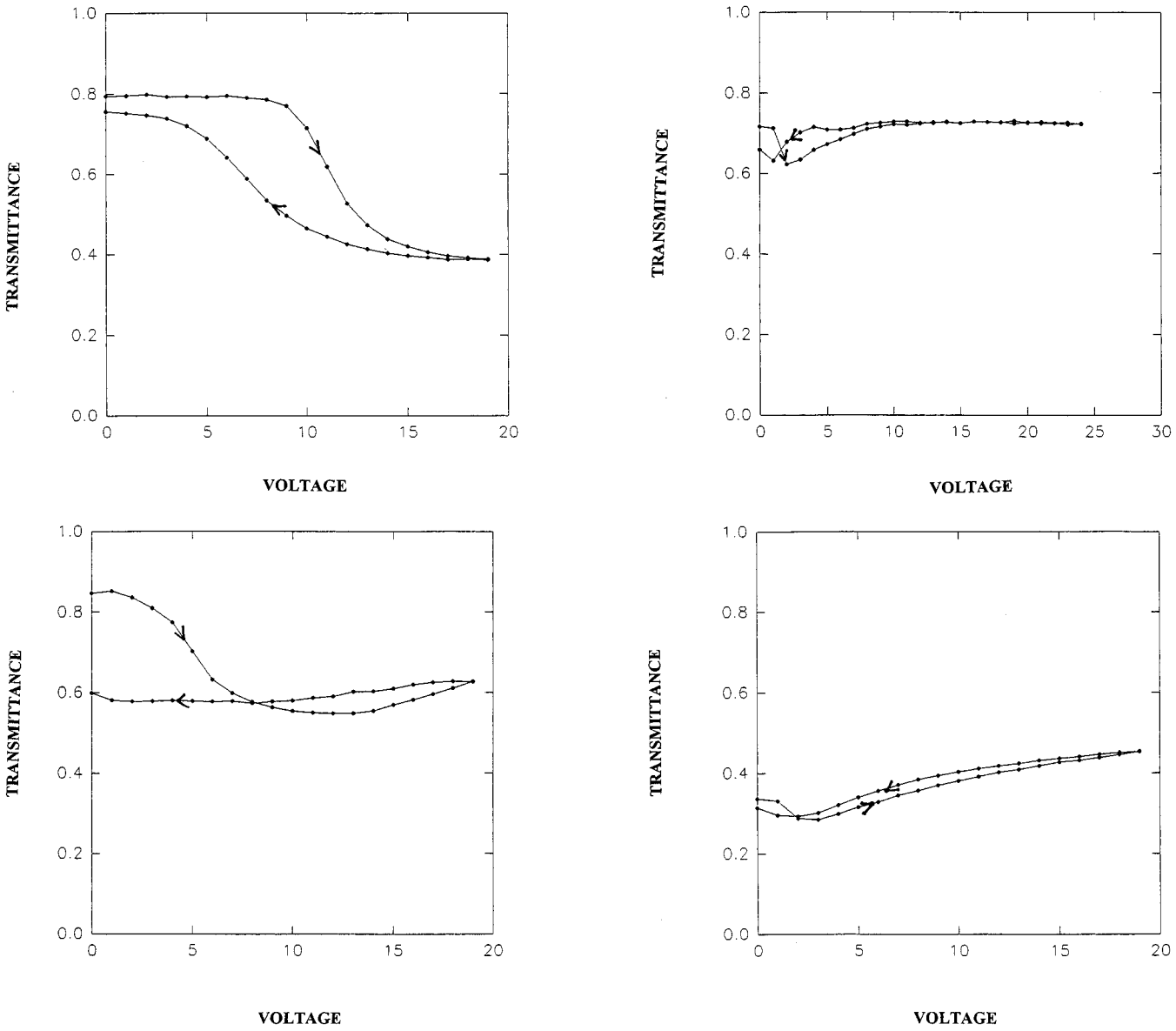

Figure 10. Electrooptic properties of a reverse mode cell of 15 μm thick containing polymer stabilized liquid crystals of **BABB6** polymerized at in **E48** at (a, top left) 28, (b, bottom left) 75, (c, top right) 95, and (d, bottom right) 140 °C.

electrooptic response of polymer-stabilized liquid crystals due to p(**BABB6**) is shown in Figure 10. Figure 10a shows the electrooptic response due to the fibrous morphology of p(**BABB6**) obtained by polymerizing **BABB6** at 28 °C. The general characteristic of the cell are similar to reverse-mode cells of **BAB6** with threshold voltage of about 9 V and a contrast of 0.4. The cell exhibited a steeper electrooptic curve with a large hysteresis. The electrooptic curve of p(**BABB6**) polymerized at 75 °C (Figure 10b), however, is unlike the response of the conventional reverse-model cell. The cell exhibits a low threshold voltage of 2 V with large hysteresis. Moreover it shows the tendency to become clear after about 15 V, and on decreasing the applied voltage it does not revert back to its original clear state and remains opaque. The poor performance of this cell may arise from the complex morphology consisting of beadlike network interspersed with platelike structures. This trend in performance continues when the cell is polymerized at slightly higher temperature. Figure 10c shows the electrooptic response of the reverse-mode cell containing **BABB6** polymerized at 95 °C. This cell shows little evidence of switching. The cell decreases in its transparency slightly by about 10% at 1 V and regains its transparency with further increase in the applied voltage. On decreasing the voltage applied it goes through the reverse process with a small hysteresis. On increasing the temperature of photopolymerization further, the transparency of the cell decreases dramatically, as shown in Figure 10d. On application of voltage, the cell gradually clears. Little hysteresis is observed upon removal of the applied voltage.

Increasing the temperature of polymerization of **BABB6** monomers causes a corresponding increase in the amount of platelike structures along with the decrease in the fiberlike character to beaded structures. This increase in platelike character is responsible for the unusual electrooptic response of these reverse-mode polymer-stabilized liquid-crystal cells and for decreasing the initial transparency of the cell at zero-field. On application of an electric field to these systems, due to large-pore structure causes the liquid crystals to possibly align along the direction of the applied field thereby increasing the transparency of the cell. This effect increases with increasing amounts of platelike structures. At high concentrations of plates, the elec-

trooptic response of the reverse-mode polymer-stabilized liquid crystal changes into a response which is very similar to that of the normal-mode[25] polymer-stabilized liquid-crystal cells which changes from a opaque OFF state due to scattering from the multidomain nematic state to a clear ON state because of homeotropic alignment of all the liquid-crystal molecules along the direction of applied voltage. The reverse-mode cell with platelike morphology is initially opaque due to the random orientation of the plates and changes gradually into a transparent state on increasing the applied voltage due to the possibly homeotropic orientation of the liquid crystals along the direction of applied voltage. If the platelike morphology could be manipulated such that there is an oriented network of plates, it is easily imaginable that the electrooptic properties of the cell would be very different, possibly with very high contrast.

It is noteworthy that there is a direct correlation between the morphology of the polymer network and the observed electrooptic properties of these reverse-mode PSLCs. It has been clearly demonstrated that we could obtain desired electrooptic response from these polymer-stabilized liquid crystals by manipulating the structure of the polymer network inside the cells.

Conclusions

The influence of temperature on the morphological development of PSLC permitted further insight to their structure and formation. Moreover, changes in morphology were found to cause changes in the electrooptic performance of PSLCs. A variety of morphologies (fibrous, beaded, and platelike) were fabricated by varying the monomer structure and temperature of photopolymerization, and each morphology has its unique effect on the electrooptic response of the reverse-mode cells.

Common to all of the systems studied (whether comprising fibers, beads, or plates), increasing temperature increases the size of the constituent units, and correspondingly the pores, of the polymer network. This result stems from the transition of aggregation behavior from being reaction-limited at short lengths and times to being diffusion-limited at greater lengths and times. A model was developed to explain how the characteristic dimension of the polymer network is controlled by monomer concentration and the relative rates of reaction and diffusion. Since the temperature dependence of the diffusion coefficient is much stronger than that for the reaction rate, increasing temperature leads to larger sizes. Increase in the characteristic dimension of the polymer networks was found to influence the electrooptic properties. Assuming equal anchoring strength, finer-scale networks can more tightly hold the LC director; therefore, increased network pore size is found to decrease the threshold switching voltage of devices. Change in morphology type, however, has a more significant effect on the threshold voltage than does a change in the characteristic dimension of the network. Greater orientational coupling between polymer and LC solvent was found for fibrous networks. Morphologies consisting of highly oriented fibers resulted in greater threshold voltage and switching hysteresis.

A new type of morphology was also found in those systems made from **BABB6**, a liquid-crystalline monomer containing a much longer mesogen. At higher temperatures, the polymer-rich domains may form smectic order, and a platelike morphology ensues. (At lower temperatures, the morphology is similar to that formed by other monomers). Devices made with a randomly oriented platelike morphology had the smallest threshold switching values and the weakest orientational coupling with the liquid-crystalline solvent.

Acknowledgment. The authors would like to gratefully acknowledge ALCOM Grant DMR89-20147 for providing financial support for this project.

CM9505207

(25) A normal-mode cell is made out of indium−tin oxide coated glass over. The monomer solution is photopolymerized with the application of high electric field.